Journal of Earth Science & Climatic Change

Kwata et al., J Earth Sci Clim Change 2017, 8:12
DOI: 10.4172/2157-7617.1000436

Research Article Open Access

A Mineralogy Study from Settleable Dust Samples in Mpumalanga Province, South Africa

Maphuti G Kwata[1,2], Shadung J Moja[1,2], Khuthadzo Masindi[1,2], Tlou Mashalane[1], Ongeziwe Mtyelwa[1,2] and Mafeto R Malatji[1]

[1]*Water and Environmental, Applied Geoscience, Council for Geosciences, 280 Pretoria Road, Silverton Pretoria, 0001, Republic of South Africa*

[2]*Department of Environmental Sciences, Florida Campus, University of South Africa, P.O. Box X6, Florida, 1710, USA*

***Corresponding author:** Maphuti G. Kwata, Water and Environmental, Applied Geoscience, Council for Geosciences, 280 Pretoria Road, Silverton Pretoria, 0001, Republic of South Africa, Tel: +27128411387; +27766789699; Fax: +27865132274; E-mail: mkwata@geoscience.org.za; maphuti.kwata@gmail.com

Received: Nov 29, 2017; **Accepted:** Dec 23, 2017; **Published:** Dec 29, 2017

Abstract

Exposure to asbestos fibers pose serious health problems which are exacerbated by wind currents and by rain water that transports fibers from asbestos mine dumps to nearby residential areas. Most of asbestos mine dumps in Mpumalanga Province are old, ownerless and not rehabilitated. The aim of this pilot study is to characterize the captured settleable dust samples. The two Sites, A and B which were selected for monitoring purpose are located about 20 km away from Mbombela, the capital city of the province. The South African National Dust Control Regulations (SANDCR) 827 of 2003 method was used to collect settleable dust around residential areas that are within 2 km of the asbestos mine dump sources in July 2015 and July 2016. The samples were chemically treated and characterized to identify the type of minerals present and to determine the morphological composition with an XRD and the SEM-EDS analytical techniques respectively. The XRD and SEM/EDS results at Site A confirms the presence of serpentine (26% m/m), organic (4% m/m) and quartz (31% m/m) minerals. Site B contain 35% m/m of serpentine, 10% m/m of amphibole, 37% m/m quartz, 21% m/m organic and 10% m/m fiber glass.

Other minerals detected at both sites were the calcite, k-feldspar, plagioclase, mica and smectite. The SEM/EDS analyses confirm that fiber glass, organic and amphibole are the longest particles/fibers with length of 485 µm, 100 µm and 64 µm respectively. The presence of asbestos dust around the residential areas highlights the possible environmental risk to those who are exposed.

Keywords: Old and ownerless; Rehabilitation; Asbestos dump; Settleable dust fall; SEM-EDS; XRD; Surface dust

Introduction

Mining of asbestos in South Africa started in the 1800's and ceased in 2002 because of environmental and health reasons. Large operations of asbestos mining in South Africa were in Northern Cape, Limpopo and Mpumalanga Provinces in this research their focus will be for Mpumalanga Province. Asbestos products were used for roofing of the houses and manufacturing of brake pads for vehicles [1]. Asbestos mine dumps of concern are unrehabilitated and are close to residential areas. Asbestos particles are microscopic in size and could be lifted from the ground based sources by wind erosion or during excavation processes [2]. Asbestos mine dumps have left major environmental and health problems. Even today there are people suffering from the exposure of airborne dust contaminated with asbestos dust. Airborne dust contaminated with asbestos is transported from old and ownerless asbestos mine dumps to the residential areas [3]. Even though asbestos mining was banned in South Africa, there is still illegal mining operations in the asbestos fields continuing to produce toxic dust [4]. Large quantities of asbestos in South Africa were used for building with little knowledge about the nature of the commodity. The asbestos mine dumps are 5 km away from the residential areas and the height is from 20m to 50m. The exposure of asbetsos mine dumps dispersed to the nearby residential areas has caused high mortality. The exposure and danger of asbestos dust was unknown people living nearby asbestos mine dumps started to get sick with repository disease which could not confirm the asbestos dust disease known to be mesothelium, lung cancer and asbestosis, etc. The method uses to mined asbestos was through milling, open cast, underground and crushing which contributed to exposure of asbestos to nearby residential areas through wind blowing. The purpose of the research is to monitor and measure settleable dust rates and characterized surface dust samples around some old and ownerless asbestos mine dumps in the vicinity of residential areas. The type of the samples collected are dust fall using single dust bucket unit and surface dust samples using a brush, dust pan, zipper plastic to determine the shape, size, width, length and type of asbestos detected. This paper reports the dust rates, mineralogical and morphological data after analyzing the settleable dust collected in the laboratory.

Materials and Methods

The study area, geology and sampling points

This pilot study took place in the north-eastern part of South Africa within residential areas around Nelspruit, Malelane and Badplaas towns which are within 2.0 km of the asbestos mine dump point sources Mbombela is the capital city of the Mpumalanga Province and is a grass land that is characterized by many pine trees, escarpment and mountainous scenery. The province's geology is composed of the Tjakastad and Komatipoort Group and Transvaal Super Group with

the sandstones, shale, murchison, greenstone belt and intrusive granite rocks being common [5]. Komatities often display spectacular textures of skeletal crystals (known as spinifex textures) which branch out like fern leaves. The textures and the chemical make-up of the rocks can be deduced from Komatities lavas which crystallized rapidly from very hot and probably water-rich molten magma [6]. The Barberton Greenstone Belt (BGB) is located in the Eastern part of Mpumalanga Province, and many asbestos mines are found in the BGB [5].

The study area experiences more rainfall in summer than in winter [7]. The average seasonal temperatures for autumn, winter, spring and summer are 19C, 14°C, 19°C and 22°C respectively. The predominant wind direction is from the North-East direction and wind speed at 3 m/s^{-1}.

Figure 1 shows the aerial locations of the two selected monitoring sites within residential areas that are within 2.0 km of the unrehabilitated asbestos mine dump sources.

Figure 1: The aerial view of location of the two monitoring sites.

Settleable dust sample collection, treatment and analyses

The sampling sites are free from obstacles, open to atmosphere and easily accessible in a secured yard. The samples were collected in July 2015 and in July 2016 using a single dust bucket monitoring unit that consist of a 2.3 m stand with a bird ring on top to secure the positioning of the collector. Each bucket was filled with a quarter of deionized water to trap and retain settled dust in the bucket. The units were exposed for 30 days before being collected and sample was filtered in the laboratory then dried at room temperature. The blank filter paper was weighed before and after filtration when dried out and left to stabilize overnight in a desiccator before final weighing. Settleable dust rate was calculated for each sampling sites for each month using the following formula:

$$D = \frac{W_f - W_b}{A \times 30 days} \text{---------- (1)}$$

Where:

D = Settleable particulate, $mg/m^2/day$

Wf = Filtered sample weight,

Wb = Blank filter weight, mg and

A = Sampling area, m^2

The calculation of settleable dust is expressed in milli-grams per metre square per day ($mg/m^2/day$) unit. Settleable dust rates were compared to the South African National Dust Control Regulations (SANDCR-827, 2013) acceptable limits [8].

The XRD and SEM/EDS analytical instruments were conditioned according to the CGS Mineralogy Laboratory Methods. X-Ray Diffraction data was obtained on BRUKER D8 Advance diffractometer with Cu radiation. The system is equipped with a LynxEye detector and a Ni-filter. Tape samples were mounted on dedicated filter holders or powder mounts and run in step scan mode from 2 to 70° 2θ CuK (λ=1.54060) radiation at a speed of 0.05° 2θ steps size/1 sec and generator settings of 40 kV and 40 mA. Data processing, evaluation and reporting: XRD: Phase identification is based on BRUKER DIFFRAC Plus - EVA evaluation program. Phase concentrations are determined as semi quantitative estimates (with accuracy ± 5%) using RIR (Reference Intensity Ratio) method and relative peak heights/areas proportions. SEM/EDS analysis was performed on a Leica Stereo scan 440 SEM linked to an OXFORD INCA EDS. The system is equipped with an Oxford X-Max SDD detector with 20 mm^2 active area and resolution of about 128eV for Mn Kα (5895 eV) and has the capabilities for secondary, backscattered and cathode-luminescence electron imaging, X-Ray EDS microanalysis and X-Ray element mapping. Mineral chemistry was determined by means of spot analyses at beam settings of 20kV accelerating voltage, probe current of 5.0 nA and counting time was set at 100s [9].

Sample preparation and processing

The settled dust samples on filter paper are mounted on specialized filter holders and used for both XRD and SEM investigations. Where possible, dust was extracted from the filters and analyzed by XRD as powder specimens. For SEM/EDS study, powders specimens are prepared as grain mounts. All specimens for SEM/EDS are coated with carbon to provide a conductive surface for optimum imaging and X-ray microanalysis. SEM/EDS analysis was done at ~800-1000 times magnification depending on particle size and distribution with the brightness/contrast settings adjusted to highlight the minerals of interest. The results are presented in form of backscattered electron (BE) images for each sample [10].

Results and Discussion

Settleable dust rates

Despite the dry and occasional windy sampling period, the settleable dust rates measured were lower than the residential area limit of 600 $mg/m^2/day$ (SANDC-827, 2013). Specifically, the setlleable dust rates in July 2015 were 28 $mg/m^2/day$ at Site A and 214 $mg/m^2/day$ at Site B. In July 2016, the settleable dust rates were 59 $mg/m^2/day$ at Site A and 39 $mg/m^2/day$ at Site B.

Mineralogy data

The XRD generated data show the dominant minerals in percentage mass/mass to be quartz (41%), serpentine (26%) and mica (22%) at Site A in 2015. The remaining minerals identified were K-feldspar (7%), plagioclase (6%), talc (6%), amphibole (4%) and calcite (2%). The mineralogy data in the same year at Site B are the serpentine (35%), quartz (31%), plagioclase (13%), talc (11%), feldspar (8%) and smectite (7%) [11].

Similar trends of mineral were measure in July 2016 with dominant minerals at Site A being serpentine (37%), plagioclase (23%), talc

(12%), quartz (10%) and smectite (9%). The minerals detected at Site B are serpentine (26%), plagioclase (21%), quartz (15%), mica (10%), talc (5%) and smectite (4%). Detailed data is also shown in Table 1.

Sample Sites	Calcite	K-Feldspar	Kaolinite	Plagioclase	Quartz	Serpentine	Amphibole	Mica	Talc	Smectite
Site A filter paper sample July 2015	2	7	9	16	41	26	6	22	6	-
Site A July 2016	-			23	10	37	-		12	9
Site B filter paper sample July 2015	-	8	-	13	31	35	10	10	11	7
Site B filter paper sample July 2016		21		19	15	26	-	10	5	4

Table 1: The percentage mineral composition measured at the two sites.

All the minerals found are classified as silicate except the calcite. Silicate minerals form the largest fraction (>90%) of most crustal rocks on earth [12]. The chrysotile asbestos which is part of the serpentine group is known to have been mined and milled in Mpumalanga [13]. The amphibole asbestos group was not mined in Mpumalanga Province and it could have been unintentionally exposed or released as an accessory trace mineral when core minerals such as gold were mined [14]. The economic benefits of quartz, plagioclase and k-feldspar include being used to manufacture glass ceramics and ceramics, while mica manufacture plates, radar circuit, and discs. Serpentine are used to manufacture brake pads for vehicles and amphibole is used to manufacture ceiling [15,16].

Adverse health effects associated with occupational exposure to chrysotile or serpentine asbestos mineral group include illnesses such as fibrosis (asbestosis), lung cancer and mesothelioma [17]. The recommended airborne exposure limit is 3 mg/m^3 for chrysotile averaged over a 10-hour work shift [18].

Dust containing mica may cause pneumoconiosis [19], which is an occupational lung disease and a restrictive lung disease caused by the inhalation of dust containing mica, often in mines. Exposures to relatively low concentrations of quartz may be capable of causing hilar node fibrosis [11]. This is characterized by localization of the fibrosing process to one or both pulmonary hila. This results in pulmonary hypertension and bronchial narrowing [20]. Occupational quartz dust exposure may also cause silicosis. Silicosis, a nodular pulmonary fibrosis or fibrotic lung disease that is caused by the inhalation and deposition of respirable crystalline silica particles (i.e., particles <10 μm in diameter) [21,22].

Morphological data

The SEM/EDS morphological results obtained from at Sites A and B in July 2015 samples are presented in Figures 2 and 3. The main minerals detected are the amphibole, chrysotile, quartz and organic matter at Site A and the amphibole and quartz minerals at Site B.

In a related study by Fowler and Chatfield [23], the transmission electron microscopy (TEM) and conventional phase contrast microscopy (PCM) were used to analyze surface dust samples and found asbestos fiber with >5 μm length as per USEPA in 1987 [24].

Common shapes detected include the platy shaped particles for the amphibole and chrysotile asbestos mineral particles, with granular shaped quartz and the blocky shaped organic matter.

The shapes detected was spiral/straw for amphibole and fiber glass, granular and sponge like for quartz, organic and serpentine.

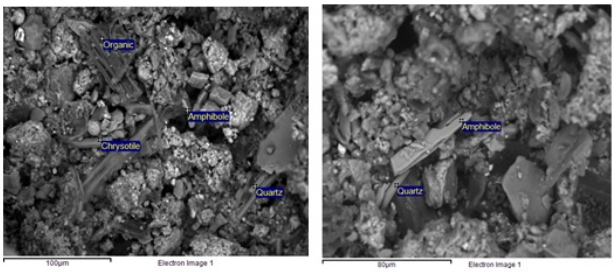

Figure 2: SEM/EDS micrograph of dust samples at Sites A and B in 2015 respectively.

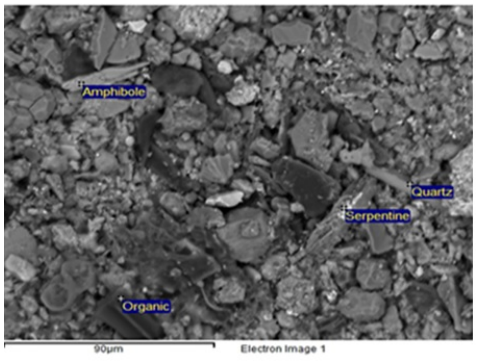

Figure 3: Representation of SEM/EDS images for Site B for July 2015.

The size characteristics lengths to width ratios of the particles/fibers are presented in Table 2 with 485:8 for fiber glass; 25:19 for amphibole; 8:5 for organic; 4:1 for amphiboles; 6:5 for feldspar; 15:4 for quartz and 5:4 for serpentine. Amphibole and serpentine particles present themselves as platy shape. Granular shaped particles are quartz and feldspars particles. Organic particles and some amphibole particles have a blocky shape as shown in Figure 2.

Tables 2 and 3 & Figure 4 shows the comparison of means between Site A and Site B and T-test was used for statistical analysis because we are comparing the means of lengths and diameter between Site A and Site B. An ANOVA test could not be used because is used for more than two variables in this research T-test was used for the statistical analysis. The T-test results for diameter for both Site A and Site B are significant which means that the results could not have been achieve by as the significant levels are mainly less than 0.05, but for lengths in both Site A and Site B we fail to reject the null hypothesis, meaning we do not have enough information to conclude that the results could not be achieved by chance.

Variables	N	Mean	Std. Deviation	Std. Error Mean
Site A Length	6	107.50	185.412	75.694
Site A Diameter	6	17.00	12.264	5.007
Site B Length	6	87.17	194.937	79.583
Site B Diameter	6	4.50	2.258	.922

Table 2: Descriptive statistics for one-sample statistics for Site A and Site B for July 2015 for the mineral particle.

Variables	Test Value = 0					
	t	Df	Sig. (2-tailed)	Mean Difference	95% Confidence Interval of the Difference	
					Lower	Upper
Site A Length	1.420	5	.215	107.500	-87.08	302.08
Site A Diameter	3.395	5	.019	17.000	4.13	29.87
Site B Length	1.095	5	.323	87.167	-117.41	291.74
Site B Diameter	4.881	5	.005	4.500	2.13	6.87

Table 3: Summary of one-sample test for the means and confidence interval for Site A and Site B for July 2016.

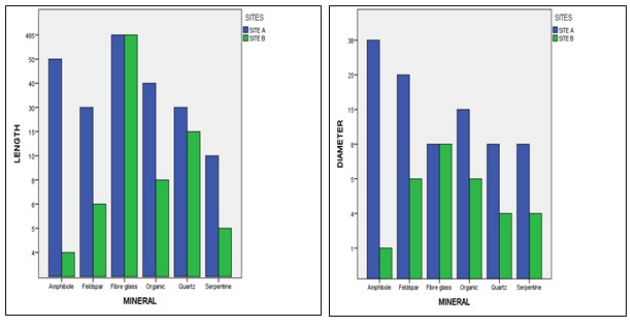

Figure 4: Comparison between length (m) and diameter (μm) for Site A and Site B for July 2015.

Figure 5, the results confirm the presence amphibole [$NaCa_2(Mg, Fe, Al)_5$ $(Al, Si)_8$ $O_{22}(OH)_2$] mineral group and serpentine [$Mg_3(OH)_4(Si_3O_5)$] other silicate minerals is quartz (SiO_2), mica [$KAI_2(Si_3AlO_{10})(OH)_2$], and plagioclase[$NaAlSi_3O$]. The biological material detected was Organic. The similar research conducted by Moja et al. shows the detected minerals amphibole and serpentine mineral group.

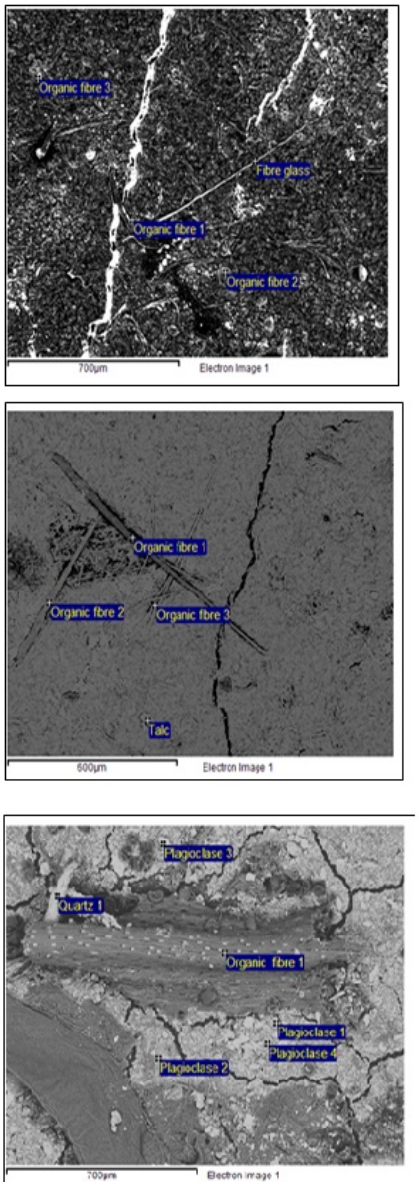

Figure 5: SEM-EDS results at Site A and Site B for July 2016.

The asbestos fibrous structures contributing to lung tumor risk appear to be long (≥ 5 μm) thin (0.4 μm) fibers and bundles, with a possible contribution by long and very thick (≥ 5 μm) complex clusters and matrices. Potency appears to increase with increasing length, with structures longer than 40 μm being about 500 times more potent than structures between <5 μm and 40 μm in length. The structures 55 μm

in length do not appear to make any contribution to lung tumor risk as studied by Bernstein et al.

Figure 5 shows that no asbestos silicate minerals were detected but quartz [SiO_2], plagioclase [$NaAlSi_3O_8$] and organic fiber were detected. The size of the mineral detected ranged from 600 µm to 700 µm semi-rectangular and shapes detected spiral and clay powder.

The size characteristics lengths to width ratios of the particles/fibers are presented in Tables 4 and 5 with 25:19 for amphiboles; 5:4 for chrysotile, 15:4 for quartz and 8:5 for organic fiber for July 2016. Amphibole and serpentine particles present themselves as platy shape. Granular shaped particles are quartz and feldspars particles. Organic particles and some amphibole particles have a blocky shape as shown in Figure 5.

Tables 4 and 5 and Figure 6 shows the comparison of means between Site A and Site B and T-test was used for statistical analysis because we are comparing the means of lengths and diameter between Site A and Site B. An ANOVA test could not be used because is used for more than two variables in this research T-test was used for the statistical analysis. The means between Sites A and B shows that Site A mean show that the results are significant and could not have been achieve by chance significance as the significant levels are mainly less than 0.05, only Site A diameter the significant levels are 0.07 slightly above the significant level.

Variables	N	Mean	Std. Deviation	Std. Error Mean
Site A Length	4	16.25	8.539	4.270
Site A Diameter	4	10.50	7.681	3.841
Site B Length	4	8.00	4.967	2.483
Site B Diameter	4	3.50	1.732	.866

Table 4: Descriptive statistics for one-sample statistics for Site A and Site B for July 2016 for the mineral particle.

Variables	Test Value = 0					
	t	Df	Sig. (2-tailed)	Mean Difference	95% Confidence Interval of the Difference	
					Lower	Upper
Site A Length	3.806	3	0.032	16.250	2.66	29.84
Site A Diameter	2.734	3	0.072	10.500	-1.72	22.72
Site B Length	3.222	3	0.049	8.000	0.10	15.90
Site B Diameter	4.041	3	0.027	3.500	0.74	6.26

Table 5: Summary of one-sample test for the means and confidence interval for Site A and Site B for July 2016.

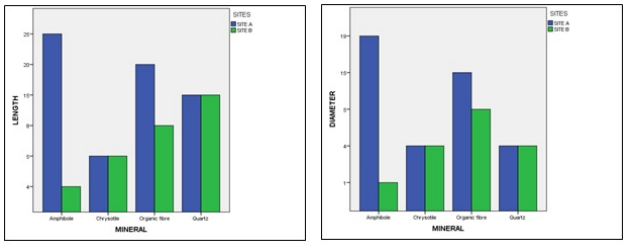

Figure 6: Comparison between length (m) and diameter (µm) for Site A and Site B for July 2016.

Conclusion

The settleable dust rates are below the residential limits of 600 mg/m^2/day. The elemental compositions together with the morphological features were used to distinguish one mineral from others. Common minerals associated with dust such as quartz, mica, K-feldspar, kaolinite, calcite and smectite were detected. All the mean are below 0.05% and only Site A diameter the distribution is not significant with 0.072%. The Site A has more mean which are far from Site B. The presence of significant levels of asbestos-form minerals such as serpentine and amphibole is of concern. These mineral types will continue to be a problem until all asbestos mine dumps are rehabilitated.

Acknowledgements

This research work was supported by the Council for Geoscience (CGS) and Department of Minerals and Resources (DMR). All SEM-EDS and XRD analyses were done at the CGS laboratories. Lerato Sebesho and Andries Somo are acknowledged for assisting during field work. Sihle Sogayise for his contribution to the stastics analysis.

References

1. Abratt R, Vorobiof D, White N (2002) Asbestos and Mesothelioma in South Africa. Lung Cancer 45: S3-S6.
2. Gosen BS (2010) Reported historic asbestos mines, historic asbestos prospects and other natural occurrences of asbestos in Oregon and Washington. USGS Open File Report 2010-1041.
3. Felix MA, Leger JP, Ehrlich RI (1994) Three minerals, three epidemic – Asbetsos mining and diseases in South Africa 265-285.
4. Kahn T (2013) Sufferers in Lonely Battle with Asbestos-related Diseases.
5. Ward JH, Wilson MG (1998) Gold outside the Witwatersrand basin. In: Wilson, M.G.C. and Anhaeusser, C.R. (editors), The Mineral Resources of South Africa, Handbook 16, Council of Geoscience 740.
6. Ehlers DL, Vorster CJ (1998) Asbestos. In: Wilson, M. G. C and Anhaeusser, C. R (edn.) The mineral resources of South Africa, Handbook Council for Geosciences 16: 740.
7. Stats SA (2015) Mid-year population estimates, Statistics South Africa.

8. South African National Dust Control Regulations (SANDCR), no 827 (2013).
9. Brime C (1985) The accuracy of X-ray diffraction method for determining mineral mixtures. Mining Management 49: 531-538.
10. Atanasova M (2016) The scanning electron microscopy mineralogy laboratory method. Council for Geosciences.
11. Seaton A, Cherrie JW (1998) Quartz exposures and severe silicosis: A role for the hilar nodes. Occupational & Environmental Medicine 55: 383–386
12. Marshall CP, Fairbridge RW (2001) Encyclopedia of Geochemistry (Encyclopedia of Earth Sciences Series), Springer, NY, USA.
13. Moja SJ, Kwata MG, Sebesho LM, Masindi KG, Mtunzi F (2016) Characterization of surface and trapped dust samples Collected around human settlements that are in the vicinity of old mine tailings in Mpumalanga Province, South Africa. J Earth Sci Clim Change 7: 1-7.
14. Visser DJ (1989) The geology of South Africa Geological Map of South Africa, 1997, Council for Geoscience Explanation: Geological Map.
15. Clayton GD (1981) Patty's industrial hygiene and toxicology, 2A, 2B, 2C, Toxicology, 3rd New York: John Wiley Sons, NY, USA. pp: 1671.
16. Jee MJ (2003) Environmental Assessment/FONSI for Sterile Talc Powder, Food and Drug Administration Center for Drug Evaluation and Research.
17. World Health Organization (1998) Environmental Health Criteria 203: Chrysotile Asbestos, Geneva, Switzerland.
18. National Institute of Occupational Safety and Health (NIOSH) (1978) Annual report on occupational safety and health under Public Law 91-596.
19. Zinman C, Richards GA, Murray J, Phillips JI, Rees DJ, et al. (2002) Mica dust as a cause of severe pneumoconiosis. American Journal of Industrial Medical 41: 139–144.
20. Yacoub MH, Thompson VC (1971) Chronic idiopathic pulmonary hilar fibrosis a clinicopathological entity. Thorax 26: 365-375.
21. Cox-Ganser JM, Burchfield CM, Fekedulegn D, Andrew ME, Ducatman BS (2009) Silicosis in lymph nodes: The canary in the miner. Journal of Occupational Environmental Medical 51: 164 -169.
22. Ziskind M, Jones RN, Weill H (1976) Silicosis. American Review of Respiratory Disease 113: 643–665.
23. Fowler DP, Chatfield EJ (1997) Surface sampling for asbetsos risk assessment. Annual Occupational Hygiene 41: 279-286.
24. United States Environmental Protection Agency (1987) 40 CFR Part 763 Appendix A: Asbestos containing materials in schools: Final rule and notice. Federal Register 52: 41870-41893.